Analysis of Delay Distribution and Rate Control over Burst-Error Wireless Channels

Joongoo Lee*, Hyungkeuk Lee** *Regular Members*, Sanghoon Lee** *Lifelong Member*

ABSTRACT

In real-time communication services, delay constraints are among the most important QoS (Quality of Service) factors. In particular, it is difficult to guarantee the delay requirement over wireless channels, since they exhibit dynamic time-varying behavior and even severe burst-errors during periods of deep fading. Channel throughput may be increased, but at the cost of the additional delays when ARQ (Automatic Repeat Request) schemes are used. For real-time communication services, it is very essential to predict data deliverability. This paper derives the delay distribution and the successful delivery probability within a given delay budget using a priori channel model and a posteriori information from the perspective of queueing theory. The Gilbert-Elliot burst-noise channel is employed as an a priori channel model, where a two-state Markov-modulated Bernoulli process ($MMBP_2$) is used. For a posteriori information, the channel parameters, the queue-length and the initial channel state are assumed to be given. The numerical derivation is verified and analyzed via Monte Carlo simulations. This numerical derivation is then applied to a rate control scheme for real-time video transmission, where an optimal encoding rate is determined based on the future channel capacity and the distortion of the reconstructed pictures.

Key Words : delay distribution, real-time service, wireless channel, channel model, queueing analysis, MMBP

Ⅰ. INTRODUCTION

Real-time multimedia communication services, such as interactive visual conferences, over wireless channels have recently become popular in the ubiquitous world. At the decoder, each access unit must arrive in the decoder buffer prior to decoding. Otherwise, over-delayed data will be lost due to decoder buffer underflow, which may lead to a severe degradation in quality. On the other side, a wireless channel exhibits a much narrower and time-varying bandwidth compared to a wired one. Under these limitations, real-time multimedia communication over dynamic wireless channels has been dealt with as a challenging issue in terms of guaranteeing QoS under a delay constraint[1].

Fig. 1 shows a simplified example of video transmission systems over the wireless channel. In the system, a video encoder is assumed to be installed on the transmitter side, and encoded data units are transmitted from the encoder buffer over the wireless channel. When a data unit, the $(N_q+1)^{th}$ unit in Fig. 1, is delivered to the queue, N_q data units are on the system. For a given channel dynamics, it is important to estimate the possibility of data delivery within a delay constraint T_{RT} for the arrival data unit.

The Gilbert-Elliot channel[2] has been widely used as an a priori channel model generating burst-errors and exhibits simplicity in analysis[3][4]. The authors focused on calculating channel capacity and on deriving an error-free run distribution[2]. Similar channel models were employed to solve rate control problems wherein these models were utilized to

※ 본 연구는 지식 경제부 및 정보통신 연구진흥원의 대학 IT연구센터 지원사업의 연구결과로 수행되었음 (IITA-2009-(C1090-0902-0011))
* 삼성전자 정보통신총괄 (jglee9@hotmail.com), ** 연세대학교 무선네트워크 연구실 (punktank@yonsei.ac.kr, slee@yonsei.ac.kr)
논문번호 : KICS2009-01-032, 접수일자 : 2009년 1월 29일, 최종논문접수일자 : 2009년 4월 21일

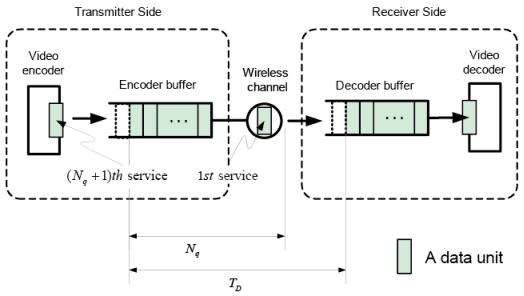

Fig. 1 A simple queing model for use in video transmission systems.

predict the future channel state[1]. However, previous studies in which the Gilbert-Elliot channel was used only focused on the prediction of the future channel state, calculation of moments, channel capacities and so on, and not on the exact delay distribution.

In this paper, we present a framework for obtaining the delay distribution at an arbitrary time instance when a priori channel model and a posteriori information are given. For the exact derivation, a three-state version of the Gilbert -Elliot channel is expressed to derive an exact delay distribution, and a new Markov chain explaining state transitions between service-starting (or service-ending) states is determined. For demonstrating the effectiveness of the numerical analysis, the expected channel capacity associated with the delay distribution and the service probability are obtained.

Ⅱ. QUEUEING ANALYSIS

In the queuing system, it is assumed that the arrival times are i.i.d. according to a general distribution, the single server employs a Gilbert-Elliot burst-noise channel with the two-state Markov-modulated Bernoulli process ($MMBP_2$), and the buffer size is infinite. The queueing system is simply denoted as $G/MMBP_2/1/\infty$.

2.1 Channel Model

The Gilbert-Elliot channel is employed[2] as an a priori wireless channel model, to predict future behavior. This model has been found to be widely suitable for generating burst-errors and exhibits simplicity in analysis. Its state transition diagram is

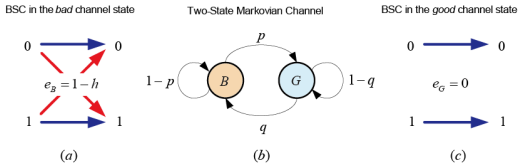

Fig. 2 Two-state Gilbert-Elliot burst-noise channel.

shown in Fig. 2 (b) where B and G indicate bad and good channel states, and p and q are the state transition probabilities. The state transition probability matrix $\boldsymbol{P}$ is then given by

$$\boldsymbol{P} = \begin{bmatrix} p_{BB} p_{BG} \\ p_{GB} p_{GG} \end{bmatrix} = \begin{bmatrix} 1-p & p \\ q & 1-q \end{bmatrix}. \quad (1)$$

The two-state Markov chain modulates the channel behavior with a transmission crossover probability, i.e., the error probability varies according to the time-varying channel state. As shown in Fig. 2 (a) and (c), the row vector $\boldsymbol{e}$ of the crossover probability is given by

$$\boldsymbol{e} = [e_B, e_G] = [1-h, 0] \quad (2)$$

In the bad channel state, each transmission makes an error with the probability $(1-h)$, while no error occurs in the good channel state. Thus, the dynamic behavior of the wireless channel is parameterized by three values, p, q and h (h = 0.5).

The states in Fig. 2 can be jointly expressed as Fig. 3 (a). The joint states are expressed by the notations $\{B\downarrow, B\uparrow, G\uparrow\}$ where the symbols $\uparrow$ and $\downarrow$ indicate success and failure of a transmission, respectively. The state transition probability matrix $\boldsymbol{P_G}$ is then given by

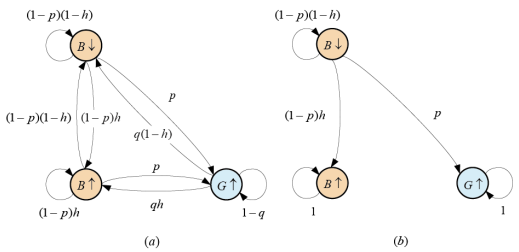

Fig. 3 (a) Three-state version of the channel model shown in Fig. 2, (b) its new version having two-absorbing states.

$$\boldsymbol{P}_G = \begin{bmatrix} (1-p)(1-h) & (1-p)h & p \\ (1-p)(1-h) & (1-p)h & p \\ q(1-h) & qh & 1-q \end{bmatrix} \quad (3)$$

The state transition probability is calculated under the assumption that channel behavior depends only on the current channel state[2].

2.2 Service Time Distribution

T_D is the sum of the service times for (N_q+1) data units including the pre-arrival $N_q$data units and the arrival data unit as shown in Fig. 1. To obtain T_D, it is necessary to find each service time $\tau(n)$ for $n=1,2,\cdots,N_q+1$. Its service time can be measured by counting the number of time slots that are passed until it reaches the first success state $\{\uparrow\}$. In order to calculate the service time statistically, a state transition probability matrix $\boldsymbol{P}_{G,A}$ is defined by

$$\boldsymbol{P}_{G,A} = \begin{bmatrix} (1-p)(1-h) & (1-p)h & p \\ 0 & 1 & 0 \\ 0 & 0 & 1 \end{bmatrix} \quad (4)$$

as shown in Fig. 3 (b).

Fig. 4 depicts a conceptual example in which the state transition matrixes $\boldsymbol{P}_A$ and $\boldsymbol{P}_{G,A}$ are utilized, where the service for a data unit starts to be served at time 0 and is finished at time t along the bold-faced line. As long as the channel still belongs to the $B\downarrow$ state, the data unit is not successfully delivered and the state transition occurs with the transition matrix $\boldsymbol{P}_{G,A}$.

2.3 The PMF of the n^{th} service

Let $P[\tau(n)=t]$ be the probability that the n^{th} service, i.e., the n^{th} data unit in the queue, begins to be served at time 0 and the process is finished at time $\tau(n)$. It can be obtained as follows. Let $\pi(t,n)$ be the row vector of the state probability at time slot t for the n^{th} service and be defined as $\pi(t,n) \equiv [\pi_{B\downarrow}(t,n), \pi_{B\uparrow}(t,n), \pi_{G\uparrow}(t,n)]$.

From the definition of $\boldsymbol{P}_A$ and $\boldsymbol{P}_{G,A}$, $\pi(1,n)=\pi(0,n)\cdot\boldsymbol{P}_G$, $\pi(2,n)=\pi(0,n)\cdot\boldsymbol{P}_G\cdot\boldsymbol{P}_{G,A}$ and so on. Generally,

$$\pi(t,n) \equiv \pi(0,n)\cdot\boldsymbol{P}_G\cdot\boldsymbol{P}^{t-1}{}_{G,A},\ t=1,2,\cdots \quad (5)$$

where $\pi(0,n)$ is the starting state for the n^{th} service, i.e., the n^{th} data unit, under the assumption that each service starts from the time slot index $t=0$ and might end at $t=1,2,\cdots$. If the service time for the n^{th} data unit is $t=1$, the initial state at $t=0$ moves to one of two states $\{B\uparrow, G\uparrow\}$ at time $t=1$. If the service is finished at time t, the state $\{B\downarrow\}$ occurs repeatedly until $t-1$ and makes a final transition to one of two states $\{B\uparrow, G\uparrow\}$ at t. Thus, $\boldsymbol{P}_G\cdot\boldsymbol{P}_{G,A}^{t-1}$ is given by

$$\begin{bmatrix} \beta^t & \frac{h(1-p)(1-\beta^t)}{1-\beta} & \frac{p(1-\beta^t)}{1-\beta} \\ \beta^t & \frac{h(1-p)(1-\beta^t)}{1-\beta} & \frac{p(1-\beta^t)}{1-\beta} \\ \frac{q\beta^t}{1-p} & \frac{qh(1-\beta^t)}{1-\beta} & \frac{h(1-p)(1-p-q)+p(1-p-q\beta^t)}{(1-p)(1-\beta)} \end{bmatrix} \quad (6)$$

where $\beta=(1-p)(1-h)$. From (5), $\pi_{B\downarrow}(t,n)$ becomes the probability that the channel makes state-transitions only to state $B\downarrow$ during $[0,t]$ for the given initial state probability $\pi(0,n)$. Thus, $\pi_{B\downarrow}(t,n)$ can be expressed by

$$\begin{aligned} &\sum_{\forall S} P[S(t,n)=B\downarrow,\cdots,S(1,n)=B\downarrow | S(0,n)=S']\pi_{S'}(0,n) \\ &= P_G P_{G,A}^{t-1}(0,0)\pi_{B\downarrow}(0,n) + P_G P_{G,A}^{t-1}(1,0)\pi_{B\uparrow}(0,n) \\ &+ P_G P_{G,A}^{t-1}(2,0)\pi_{G\uparrow}(0,n) \\ &= \pi_B(0,n)\beta^t + \pi_G(0,n)\frac{q\beta^t}{1-p} \end{aligned} \quad (7)$$

where $S(t,n)$ indicates the channel state at time t for the n^{th} service and $S'\in\{B\downarrow, B\uparrow, G\uparrow\}$. Hence, from (4) and (7), the pmf $P[\tau(n)=t]$ of the n^{th} service time $\tau(n)$ is obtained by

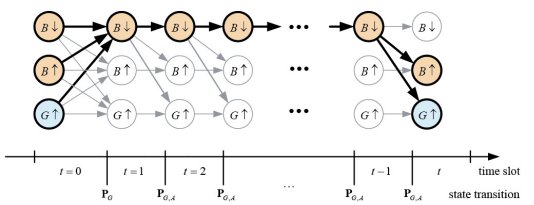

Fig. 4 State transitions for a single service.

$$P[\tau(n)=t]=\begin{cases}\pi_{B\uparrow}(1,n)+\pi_{G\uparrow}(1,n), & t=1\\ \pi_{B\uparrow}(t-1,n)\{P_{G,A}(0,1)+P_{G,A}(0,2)\}, & t=2,3,4\end{cases} \tag{8}$$

Let $\pi_A(n)$ be the state probability as $t\to\infty$. Since $0\le\beta<1$ in (6), β^t becomes zero as $t\to\infty$. Thus,

$$\pi_A(n)=\lim_{t\to\infty}\pi(t,n)=\pi(0,n)\boldsymbol{P_G}\boldsymbol{P}_{G,A}^{\infty}=[0,\pi_{B\uparrow}(n),\pi_{G\uparrow}(n)] \tag{9}$$

From (9), it can be seen that the first column of $\pi_A(n)$ becomes zero as $t\to\infty$. Thus, the final state will be absorbed into either the $B\uparrow$ state or the $G\downarrow$ state.

2.4 The state transition matrix for the service ending state

$\pi(0,n)$ in (9) can be substituted by $\pi_A(n-1)$, and yields

$$\pi_A(n)=\pi_A(n-1)\boldsymbol{P_G}\boldsymbol{P}_{G,A}^{\infty}. \tag{10}$$

Thus, $\boldsymbol{P_G}\boldsymbol{P}_{G,A}^{\infty}$ acts similar to a state transition probability matrix between the two ending states $\pi_A(n-1)$ and $\pi_A(n)$. To deal with this state transition, the state transition probability matrix $\boldsymbol{P}_{G,S}$ is defined using (16) as

$$\begin{aligned}\boldsymbol{P}_{G,S}&=\begin{bmatrix}P_G P_{G,A}^{\infty}(2,2) & P_G P_{G,A}^{\infty}(2,3)\\ P_G P_{G,A}^{\infty}(3,2) & P_G P_{G,A}^{\infty}(3,3)\end{bmatrix}\\&=\frac{1}{1-\beta}\begin{bmatrix}(1-p)h & p\\ qh & p(1-h)+(1-q)h\end{bmatrix}.\end{aligned} \tag{11}$$

Assuming that a transition occurs at the end of each service interval, a new Markovian chain (shown in Fig. 5) can be considered. In such a case, two states $\{B_A, G_A\}$ are newly devised to represent service-ending states virtually (B_A for an ending with $B\uparrow$ and G_A for an ending with $G\uparrow$).

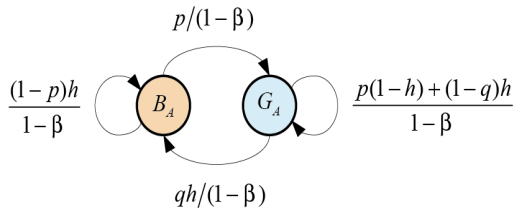

Fig. 5 Service-ending (or, equally, service-starting) state transition diagram.

Generally, using the law of total probability,

$$\begin{aligned}P[\tau(n)=t]=&P[\tau(n)=t|S(0,n)=B]\,P[S(0,n)=B]\\&+P[\tau(n)=t|S(0,n)=G]\,P[S(0,n)=G].\end{aligned} \tag{12}$$

Due to the memoryless property of a Markov chain (including Fig. 5), each service time only depends on its initial state, and formally,

$$P[\tau_{S'}=t]=P[\tau(n)=t|S(0,n)=S'],\ S'\in\{B,G\}.$$

The pmf for $\tau(n)$ in (12) can be then rewritten as

$$\begin{aligned}P[\tau(n)=t]=&P[\tau_B=t]\,P[S(0,n)=B]\\&+P[\tau_G=t]\,P[S(0,n)=G]\end{aligned} \tag{13}$$

Since $P[\tau(n)=t]$ is independent on n, set to $n=1$. By applying $P[\tau_S=t]$ to (8),

$$\begin{cases}P[\tau_B=t]=(1-\beta)\beta^{t-1}, & t\ge 1\\ P[\tau_B=t]=\begin{cases}1-q(1-h), & t=1\\ \dfrac{q}{1-p}(1-\beta)\beta^{t-1}, & t\ge 2\end{cases}\end{cases} \tag{14}$$

and, generally,

$$\begin{aligned}P[S(0,n)=S]=&\sum_{S'\in\{B,G\}}P[S(0,n)=S|S(0,1)=S']\\&\cdot P[S(0,1)=S']\end{aligned}$$

where $P[S(0,n)=S|S(0,1)=S']$ is given by $\boldsymbol{P}_{G,S}^{n}$. From (11), $\boldsymbol{P}_{G,S}^{n}$ is given by

$$\boldsymbol{P}_{G,S}^{n}=\frac{1}{p+qh}\begin{bmatrix}qh+p\alpha^n & p-p\alpha^n\\ qh-qh\alpha^n & p+qh\alpha^n\end{bmatrix}. \tag{15}$$

Thus, the n^{th} service time $\tau(n)$ is entirely dependent on the initial channel state $S(0,1)$ at the instant at which the delay measurement starts. The conditional pmf of the n^{th} service time is given by

$$\begin{bmatrix}P[\tau(n)=t|S(0,1)=B]\\ P[\tau(n)=t|S(0,1)=G]\end{bmatrix}=\boldsymbol{P}_{G,S}^{n}\begin{bmatrix}P[\tau_B=t]\\ P[\tau_G=t]\end{bmatrix}. \tag{16}$$

2.5 Delay distribution and service probability

Tthe queueing delay T_D is the sum of the service

times for N_q+1 data units including the arrival data unit. The distribution of $\tau(n)$ is entirely dependent on the starting state $S(0,n)$. Let N_B be the number of services starting from the state B and N_G be the number of services starting from the state G. For N_q+1 services, $N_B+N_G=N_q+1$. T_D then becomes

$$T_D=\sum_{n=1}^{N_q+1}\tau(n)=\sum_{i=1}^{N_B}\tau_{B,i}+\sum_{j=1}^{N_G}\tau_{G,j}.$$

The generating function $G_{T_D}(z)$ of T_D becomes

$$G_{T_D}(z)=G_{\tau_B}^{N_B}(z)\,G_{\tau_G}^{N_G}(z)=G_{\tau_B}^{N_B}(z)\,G_{\tau_G}^{N_q+1-N_B}(z). \quad (17)$$

Since N_B and N_G are random variables, (17) becomes

$$G_{T_D}(z)=G_{N_B}\left(G_{\tau_B}(z)\right)G_{N_G}\left(G_{\tau_G}(z)\right) \quad (18)$$

where $G_{\tau_B}^{N_B}(z)=G_{N_B}\left(G_{\tau_B}(z)\right)$ and $G_{\tau_G}^{N_G}(z)=G_{N_G}\left(G_{\tau_G}(z)\right)$. $G_{\tau_B}(z)$ and $G_{\tau_G}(z)$ can be derived simply through the z-transform of (14) as

$$G_{\tau_B}(z)=\frac{(1-\beta)z}{1-\beta z} \quad (19)$$

and

$$G_{\tau_G}(z)=(1-q(1-h))z+\frac{q(1-h)(1-\beta)z^2}{1-\beta z}. \quad (20)$$

Given a sequence of N_q+1 services, let $\hat{\pi}(N_B,N_G)$ be the probability vector, indicating that N_B and N_G services occur during the N_q services: $\hat{\pi}(N_B,N_G)=\left[\widehat{\pi_B}(N_B,N_G),\widehat{\pi_G}(N_B,N_G)\right]$ where each column $\hat{\pi}_{S\in\{B,G\}}(N_B,N_G)$ corresponds to the case where the service-sequence ends with S-starting service (each sequence ends with B- or G-starting service). Using the memoryless property of transitions between service-ending states, $\hat{\pi}(N_B,N_G)$ can be expressed by $\hat{\pi}(N_B-1,N_G)$ and $\hat{\pi}(N_B,N_G-1)$.

Suppose the next service transition occurs with the B-starting service from $\hat{\pi}(N_B-1,N_G)$. The service sequence probability then becomes

$$\hat{\pi}(N_B,N_G)=\hat{\pi}(N_B-1,N_G)\boldsymbol{P}_{G,S}[1\,0]^T.$$

Similarly, the service sequence probability from the state $\hat{\pi}(N_B,N_G-1)$ with the G-starting service becomes

$$\hat{\pi}(N_B,N_G)=\hat{\pi}(N_B,N_G-1)\boldsymbol{P}_{G,S}[0\,1]^T.$$

Then, $\hat{\pi}(N_B,N_G)$ becomes

$$\left[\hat{\pi}(N_B-1,N_G)\boldsymbol{P}_{G,S}\begin{bmatrix}1\\0\end{bmatrix}\ \hat{\pi}(N_B,N_G-1)\boldsymbol{P}_{G,S}\begin{bmatrix}0\\1\end{bmatrix}\right]. \quad (21)$$

Using (21), $\hat{\pi}(N_B,N_G)$ can be recursively derived. The pmf $P[N_B=n|N_q]$ can be obtained by the recursive expression with the initial state probability $\pi(0,1)$. The generating function can be calculated by

$$G_{N_B}(z)=\sum_{n=0}^{N_q+1}z^nP[N_B=n|N_q],$$

and $G_{T_D}(z)$ can be calculated from (18), (19) and (20). The pmf of the queueing delay T_D then becomes

$$P[T_D=t]=\frac{1}{t!}\frac{d^t}{dz^t}G_{T_D}(z)|_{z=0}. \quad (22)$$

The service probability P_S is then expressed by

$$P_S=P[T_D\le T_{RT}]=\sum_{t=1}^{T_{RT}}P[T_D=t] \quad (23)$$

where T_{RT} is the real-time delay constraint.

Ⅲ. RATE CONTROL ALLOCATION

A rate control algorithm can be employed to obtain the optimal rate using feedback information for a given encoding rate and the characteristics of the wireless channel. Fig. 6 depicts a transmission system in which the current buffer occupancy and the channel state information are sent back to the encoder side. Utilizing this information, an encoding rate can be determined.

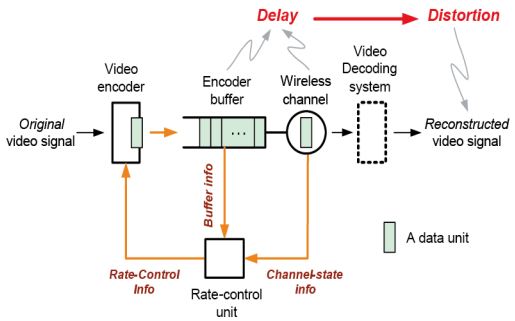

Fig. 6 A rate-controlled real-time video communication system.

3.1 Expected channel capacity

Let $C_{\max}$ be the maximum channel capacity during the delay constant when no channel error occurs, and $\pi(0,1)$ be the initial channel state probability. Let C_B (C_G) be the channel capacity at the bad (good) channel state. Then, C_B and C_G are represented by

$$\begin{bmatrix} C_B \\ C_G \end{bmatrix} = \begin{bmatrix} (1-e_B)C_{\max} \\ (1-e_G)C_{\max} \end{bmatrix} = C_{\max}(\mathbf{1}-\boldsymbol{e})^T$$

Under the assumption that no channel error occurs at the good channel state, $e_G = 0$ and $C_B = (1-e_G)C_{\max}$. The average channel capacity at time t is then given by

$$C(t) = \pi(t,1)\begin{bmatrix} C_B \\ C_G \end{bmatrix} = C_{\max}\pi(0,1)\boldsymbol{P}^t(\mathbf{1}-\boldsymbol{e})^T$$

The probability that the arrival data unit is delivered to the decoder buffer after t slots is represented by $P[T_D = t]$. The average channel capacity C for the delivery of the data unit to the decoder buffer can be written as

$$C = \sum_{t=1}^{\infty} \pi(0,1)\boldsymbol{P}^t(\mathbf{1}-\boldsymbol{e})^T P[T_D = t] \tag{24}$$

where $\boldsymbol{P}$ is given in (1), $\boldsymbol{e}$ in (2) and $\mathbf{1} = [1,1]$ Generally, $0 \le C \le C_{\max}$ and, in the discrete time domain, at most one data-unit transmission is allowed in a single slot.

3.2 Optimal rate

Due to the limited channel capacity in (40), the data rate delivered to the decoder is limited by

$$R' = \begin{cases} P_S R, & R < C/P_S \\ C, & R \ge C/P_S \end{cases} \tag{25}$$

where C is the channel capacity in (24), R is the encoding rate and R' is the data rate delivered to the decoder. Fig. 7 shows the instant receiving rate as a function of the transmission rate. The optimal transmission rate R^* required to minimize the distortion for the given R and R' can be then expressed as

$$R^* = \arg_R \min D_t'(R, R') \tag{26}$$

where D_t' t is the distortion of the reconstructed picture at the decoder.

Let $D_p(R_p)$ be the distortion (rate) at the p^{th} pixel. Suppose that the encoded data for the pixel is lost during the transmission. The distortion due to the pixel loss can be approximated by $D_{p,e} = D_p(0)$ which is equivalent to the maximum distortion with the zero encoding rate. Assume that each picture consists of N_t pixels. Simply, the average distortion D_p' per pixel can be written as

$$\begin{aligned} D_p' &= E\left[\frac{D_t'}{N_t}\right] = E\left[\frac{D_{p,c}N_c + D_{p,e}N_e}{N_t}\right] \\ &= D_{p,c}P_c + D_{p,e}P_e = D(R_p)P_c + D(0)P_e \end{aligned}$$

where P_c is given by

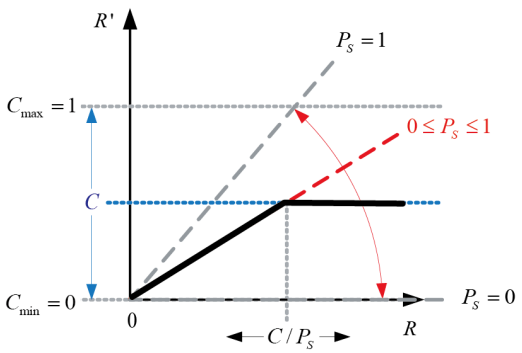

Fig. 7 The instant receiving rate according to the transmission rate.

$$P_c = \begin{cases} P_S, & 0 \le R_p \le \dfrac{C}{P_S N_t} \\ \dfrac{C}{R_p N_t}, & R_p \ge \dfrac{C}{P_S N_t} \end{cases}$$

referring to (25) and $P_e = 1 - P_c$. Assuming that the over-delayed data is regarded as lost data, the total distortion of the reconstructed picture D_t' can be written as

$$D_t' = D_{p,c} N_c + D_{p,e} N_e$$

where N_c is the number of received pixels and N_e is the number of lost pixels in a picture ($N_t = N_e + N_c$). The average distortion D_p' per pixel is given by

$$D_p' = \begin{cases} D_p(R_p) P_S + D_p(0)(1 - P_S), & 0 \le R_p \le \dfrac{C}{P_S N_t} \\ \dfrac{D(R_p) C}{R_p N_t} + D(0)\left(1 - \dfrac{C}{R_p N_t}\right), & R_p \ge \dfrac{C}{P_S N_t} \end{cases} \quad (27)$$

Using (27), the distortion per pixel of the Gaussian source is then given by

$$D_p' = \begin{cases} D_p(R_p) P_S + D_p(0)(1 - P_S), & 0 \le R_p \le \dfrac{C}{P_S N_t} \\ \dfrac{D(R_p) C}{R_p N_t} + D(0)\left(1 - \dfrac{C}{R_p N_t}\right), & R_p \ge \dfrac{C}{P_S N_t} \end{cases}. \quad (28)$$

Finally, the optimal for constructing a Gaussian picture with minimal distortion, satisfying (26), is given by

$$R_{p,G}^* = \frac{C}{P_S N_t} \quad (29)$$

and its minimum per-pixel distortion is given by

$$D_{p,G}'(R_{p,G}^*) = \sigma^2 2^{\frac{-2C}{P_S N_t}} P_S + \sigma^2 (1 - P_S).$$

Ⅳ. SIMULATION RESULTS

The formulas derived from the queueing model are verified using the Monte Carlo simulation method with a repetition time of 10^7. It can be seen that the pmf plot of the delay T_D in (34) is in good agreement with the simulation result when $N_q = 0$ and $N_q = 10$ in Fig. 8 (a) and (b). In the simulation, the channel parameters are set to $p = q = 0.05$ and $h = 0.5$ for modeling slow fading channel. Services starting from the bad channel state have less chance to be successfully completed in the following time slots due to the low success probability $h = 0.5$. This figure also shows that the pmf curve is highly dependent on the initial channel state $\pi(0,1)$.

Fig. 9 shows the service probability P_S when the real-time delay constraint is $T_{RT} = 50$ (slots) in the discrete time domain. When the queue-length is small, the service probability is almost one, i.e., the service can be completed with a very low

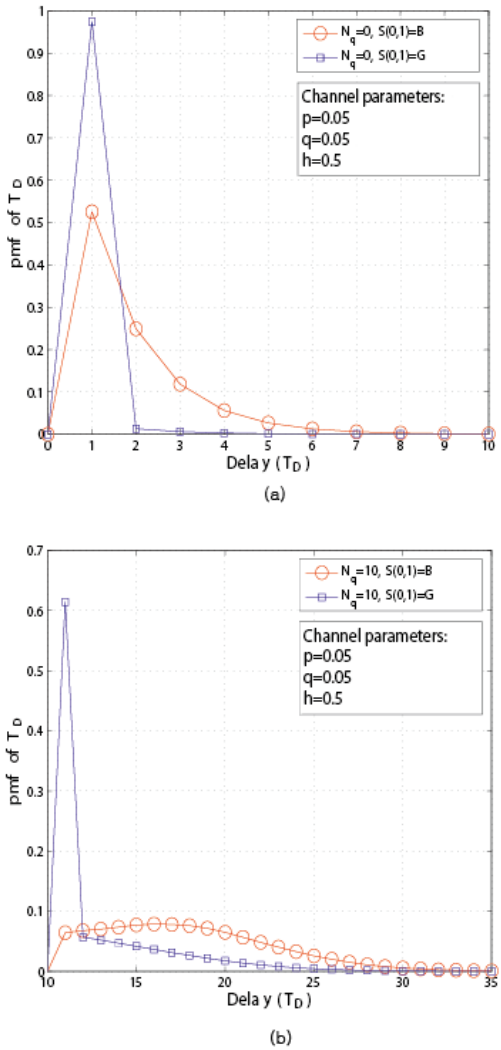

Fig. 8 The pmf of the delay according to the parameters.

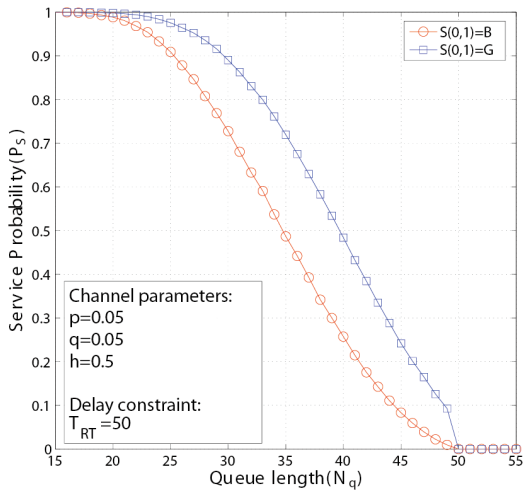

Fig. 9 The service probability according to the instant channel state and the queue-length.

probability of failure. If the queue-length becomes longer than 25, the service probability is decreased and has less chance to finish its service within the delay budget. Hence, service probability drops with increasing queue-length.

V. CONCLUSION

This paper presents a theoretical derivation for analyzing queueing behavior by means of delay and service distributions over a Gilbert-Elliot burst-noise channel. For describing the channel dynamics, the two-state Markov-modulated Bernoulli process is analyzed for the queueing system. To demonstrate the applicability of the analysis, a quality maximization problem is treated by utilizing the distortion function. The numerical analysis presented in this paper has the potential of being utilized for solving a variety of QoS optimization problems where delay constraints are major QoS factors.

REFERENCES

〔1〕 S. Aramvith, I.-M. Pao and M.-T. Sun, "A rate-control scheme for video transport over wireless channels," *IEEE Trans. Circuits Syst. Video Tech.*, vol. 11, pp. 569-580, May 2001.

〔2〕 E. N. Gilbert, "Capacity of a burst-noise channel," *Bell Syst. Tech. J.*, vol. 39, pp. 1253-1265, Sept. 1960.

〔3〕 C. C. Tan and N. C. Beaulieu, "First-order Markov modeling for the Rayleigh fading channel," *IEEE GLOBECOM '98*, Sydney, Australia, vol. 6, pp. 3669-3674, Nov. 8-12 1998.

〔4〕 Q. Zhang and S. A. Kassam, "Finite-State Markov Model for Rayleigh Fading Channels," *IEEE Trans. Commun.*, vol. 47, pp. 1688-1692, Nov. 1999.

이 준 구 (Joongoo Lee) 정회원

1999년 2월 충남대학교 전자공학과 학사졸업
2006년 2월 연세대학교 전기전자공학과 석사졸업
1999년 3월~현재 삼성전자 정보통신부문 연구원
<관심분야> 무선통신, 모바일 QoS

이 형 극 (Hyungkeuk Lee) 정회원

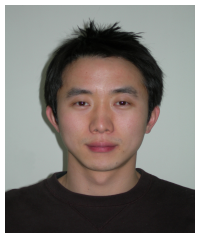

2005년 2월 연세대학교 전기전자공학과 학사졸업
2006년 8월 연세대학교 전기전자공학과 석사졸업
2006년 9월~현재 연세대학교 전기전자공학과 박사과정
<관심분야> 무선통신, 비디오통신, 최적화이론

이 상 훈 (Sanghoon Lee) 종신회원

1989년 2월 연세대학교 전자공학과 학사졸업
1991년 2월 한국과학기술원 전자공학과 석사졸업
1991년~1996년 KT 책임연구원
2000년 6월 The University of Texas at Austin 전자공학과 박사졸업
2000년~2003년 Bell Lab., Lucent Technologies 책임연구원
2003년 2월~현재 연세대학교 전기전자공학과 부교수
<관심분야> 무선통신, MIMO, 비디오통신, 최적화이론, 영상화질평가, 센서네트워크